Laser damage resistant anti-reflection microstructures in Raytheon ceramic YAG, sapphire, ALON™, and quartz.

Douglas S. Hobbs*, Bruce D. MacLeod, Ernest Sabatino III
TelAztec LLC, 15 A Street, Burlington, MA, USA 01803-3404

Thomas M. Hartnett^, Richard L. Gentilman
Raytheon Integrated Defense Systems, Mechanical Engineering Directorate
350 Lowell Street Street, Andover, MA, USA 01810

ABSTRACT

A study of the laser induced damage threshold (LiDT) of anti-reflection (AR) microstructures (ARMs) built in the end facets of metal ion doped yttrium aluminum garnet (YAG) laser gain material, has been conducted. Test samples of undoped and ytterbium-doped polycrystalline YAG produced by Raytheon Company were processed with ARMs in one surface and subjected to standardized pulsed LiDT testing at the near-infrared (NIR) wavelength of 1064nm. As received YAG samples with a simple commercial polish were also submitted to the damage tests for comparison, along with YAG samples that were treated with a single layer thin-film AR coating designed for maximum transmission at 1064nm. Additional samples of single crystal sapphire and quartz, and polycrystalline ALON™ windows were prepared with thin-film AR coatings and ARMs textures to expand the 1064nm laser damage testing to other important NIR transmitting materials. It was found that the pulsed laser damage resistance of ARMs textured ceramic YAG windows is 11 J/cm^2, a value that is 43% higher than untreated ceramic YAG windows, suggesting that ARMs fabrication removed residual sub-surface damage, a factor that has been shown to be important for increasing the damage resistance of an optic. This conclusion is also supported by the high damage threshold values found with the single layer AR coatings on ceramic YAG where the coatings may have shielded the sub-surface polishing damage. Testing results for the highly polished sapphire windows also support the notion that better surface preparation produces higher damage resistance. The damage threshold for untreated sapphire windows exceeded 32 J/cm^2 for one sample with an average of 27.5 J/cm^2 for the two samples tested. The ARMs-treated sapphire windows had similar damage thresholds as the untreated material, averaging 24.9 J/cm^2, a value 1.5 to 2 times higher than the damage threshold of the thin film AR coated sapphire windows.

Keywords: Antireflection, AR, Motheye, Microstructures, LIDT, YAG, High Power Lasers, Thin-Film AR Coatings

1. INTRODUCTION

Metal ion doped yttrium aluminum garnet (YAG) material is widely used as a gain medium in high power solid-state lasers[1,2]. Increasingly, the wide transmission bandwidth and mechanical durability of polycrystalline YAG has made its use as an infrared transparency attractive for laser targeting and sensor applications[3-7]. Raytheon has been developing ceramic YAG material to address the need for large area materials with lower costs than those that can be produced with conventional single crystal growth processes. Ceramic YAG can be produced with a greater refractive index uniformity than single crystal YAG, and can be doped in a more flexible manner to yield higher dopant concentrations or spatially varied concentrations. As solid state laser gain media becomes larger in order to scale to higher power levels, these factors will become increasingly significant.

To add optical functions such as wavelength filtering, polarization, or anti-reflection (AR) to YAG laser rods or windows currently requires the deposition of multiple layers of dissimilar thin-film materials designed to produce interference effects for light within a target wavelength band. However, these thin-film material stacks are easily damaged at laser power levels that severely limit the lifetime, output power, and reliability of a laser system. Surface relief microstructures offer an alternative to thin-film coatings for high power laser systems[9]. In standardized pulsed laser damage testing at multiple wavelengths ranging from the near UV through the long wave infrared, AR microstructures (ARMs) built in the surface of many types of materials have consistently exhibited damage thresholds 2 to 5 times higher than thin-film AR coatings[10]. For this work, the laser damage resistance of ARMs textures built in Raytheon ceramic YAG, Crystal Systems single crystal sapphire, Surmet poly-crystal ALON™, and single crystal quartz

* dshobbs@telaztec.com; phone 1 781 229-9905; fax 1 781 229-2195; www.telaztec.com
^ thomas_m_hartnett@raytheon.com; phone 1 978 470 9302; fax 1 978 470 9003

windows was compared to the damage resistance of untreated and thin-film AR coated windows using a standardized testing service provided by Quantel USA. The tests were run at a near-infrared (NIR) wavelength of 1064nm where the use of ARMs technology has the potential to significantly increase the damage threshold of pump beam integrators, gain media facets, and laser cavity components.

2. ARMs TEXTURE DESIGN MODELING

Forming ARMs textures out of the same material as a bulk optic or window eliminates the power handling and bandwidth limitations caused by the need for planar interfaces and dissimilar materials when applying conventional thin-film AR coating technology. Because both surface relief textures provide a gradual change in the refractive index at a material boundary, light can propagate through the boundary without material damage at energy levels that are much higher than that found with thin-film interference coatings. Multiple types of ARMs textures, commonly known as *Motheye* textures in the literature,[11-14] have been demonstrated to outperform AR coatings in overall light reflection suppression, operational bandwidth, field of view, polarization, environmental durability, radiation resistance, long term reliability, and power handling capacity[15-19]. For YAG laser applications the power handling capacity of ARMs technology is the main focus. Figure 1 illustrates three types of ARMs textures that can be fabricated in the end facets of a YAG laser rod to eliminate reflections over the NIR wavelength range where most metal ion dopants such as neodymium, erbium, and ytterbium produce laser emission. The features in the ARMs texture are organized in a periodic array with a spacing that is much smaller than the target wavelength to ensure that there will be no transmission loss due to diffraction. For normal incidence illumination with 1064nm wavelength light of an ARMs texture in YAG, the array spacing Λ, must be set less than 1064/1.82 =585nm (λ/n, where n is the refractive index of YAG at a wavelength λ=1064nm), to avoid diffraction. The height h of the features in the array impacts the performance bandwidth with taller structures typically operating over a wider spectral range. Feature shape is most significant for the ARMs fabrication process where lower aspect ratio, flat top profile structures can be made more uniform over larger areas in a wider range of materials. [A fourth diagram depicting a single layer thin-film AR coating is also shown in Figure 1 where the coating thickness is designed to be the target wavelength divided by four times the coating refractive index. Maximum performance is obtained when the coating refractive index matches the square root of the bulk optic refractive index].

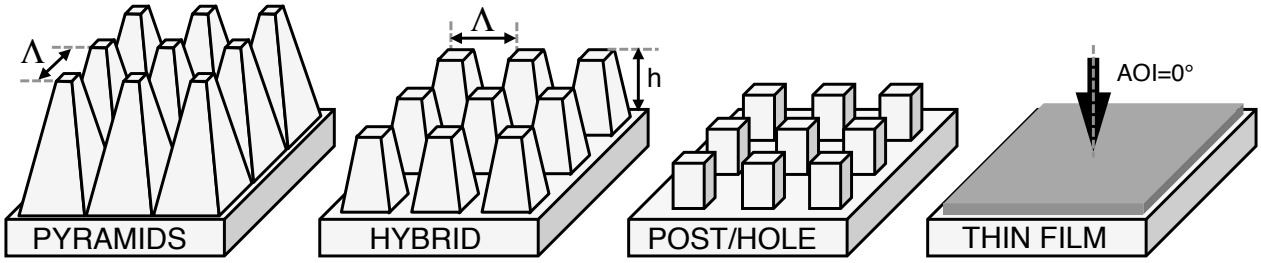

Figure 1: Diagrams representing three types of ARMs textures and a single layer AR coating.

For the YAG laser application, a more detailed prediction of the performance of the various types of ARMs textures was made through optical modeling. A three-dimensional computer model was constructed using a vector diffraction program based on rigorous coupled wave theory that solves Maxwell's equations at each layer in a stepwise approximation. Up to nine two-dimensional layers were employed to accurately model arrays of three-dimensional structures similar to those depicted in Figure 1. The library includes published data for the refractive index of YAG to properly account for dispersion. Figure 2 gives the simulation results where the predicted transmission of normally incident NIR light propagating from an air environment through the ARMs texture and into the bulk YAG material is plotted over the spectral range of from 0.9µm to 1.9µm. Cross sectional diagrams showing the dimensions for each design variant are inset in the plot. An array spacing of 500nm was set for all variants where no diffraction is possible for wavelengths longer than 905nm (this includes the pump band for ytterbium-doped YAG which is relatively wide spanning the range of from 930-960nm as can be seen in Figure 3 below).

Broad-band transmission is predicted for Motheye-type ARMs textures consisting of arrays of both linear profile (solid black curve) and sinusoidal profile (solid grey curve) pyramids. The tip of each square based cone structure is removed in the simulation to better match the structures that are typically fabricated. Notice that the height of the sinusoidal cone structures is just 80% of the height needed to attain nearly equivalent performance from linear profile structures. This

dependence on cross sectional profile becomes increasingly important for higher refractive index materials such as silicon and germanium[9,17], and for wider bandwidth applications where higher aspect ratio structures are needed. SWS-type ARMs textures consisting of an array of square profile mesas (dotted black curve), produce maximum transmission at the target design wavelength of 1030nm, but falls off more rapidly at longer wavelengths. Binary profiles perform in a manner that is equivalent to a single layer thin-film AR coating, but with the important design advantage that low reflectance can be created for materials such as fused silica or quartz where thin-film materials with the needed low refractive index (~1.2) are fragile (sol-gel) or do not exist. Hybrid ARMs textures consisting of an array of tapered posts (dashed grey curve), provide good performance at the target wavelength that decreases only slightly at longer wavelengths. With an aspect ratio just 50% higher than SWS mesas, and only 60% of the pyramid structure aspect ratio, Hybrid textures offer a good balance between ease of fabrication and performance.

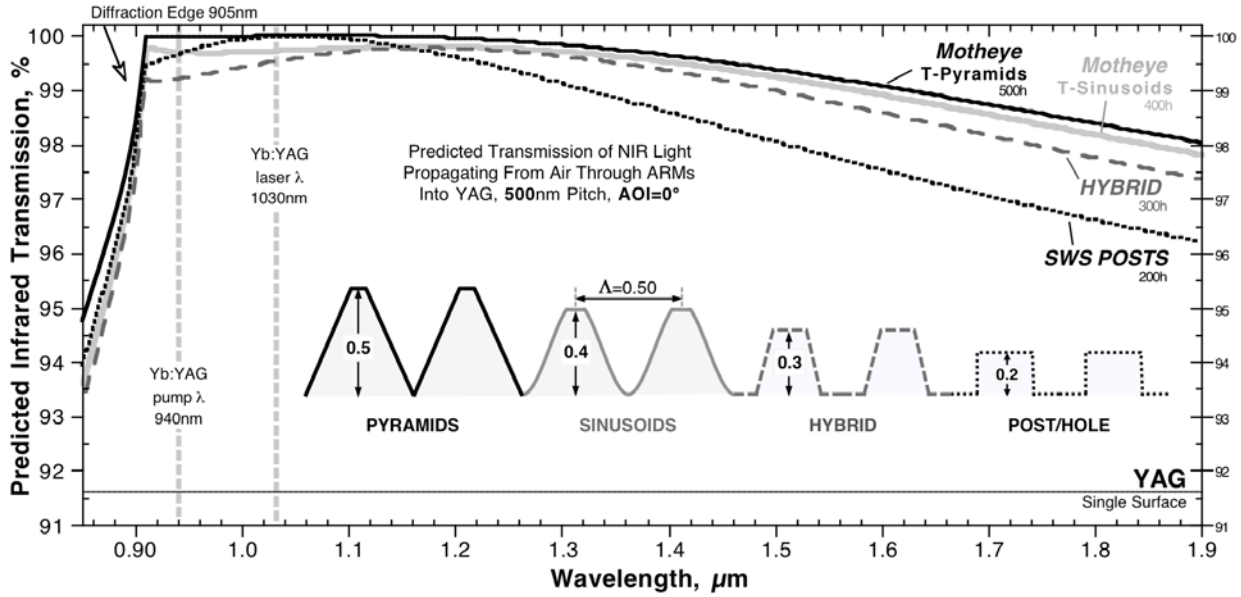

Figure 2: Predicted single surface transmission through various design ARMs textures in YAG.

3. ARMs TEXTURE FABRICATION AND MEASURED PERFORMANCE

Raytheon provided 18 samples of their ceramic YAG material doped with ytterbium, and 10 samples of their un-doped ceramic YAG. Each sample was cut and polished by Raytheon to a size of 10x10mm, 1.8 or 2.0mm thick. The transmission and reflection of each sample was measured using a grating-based NIR spectrometer operating over the wavelength range of 0.9μm to 1.7μm. Two multi-mode fiber optic cables equipped with collimating lenses were used to transmit a broad-band light source through each sample, and to return the transmitted light to the spectrometer input. A single bifurcated fiber cable was used to send and receive the broad-band light source during reflectance measurements. Transmission measurements of the YAG samples were also made in the mid-infrared wavelength range of from 1.8μm to 20μm using a Nicolet 550 FTIR spectrometer. Figure 3 shows the transmission data where the low dispersion of Yb:YAG (solid grey curve) and un-doped YAG (dashed black curve) leads to a relatively flat transmission – 83% to 84% - over the spectral range from 1μm to 4μm. Note the ytterbium absorption band centered at 0.94μm. The transmission curve represents the average of all the samples received where the transmission variation part to part was less than the measurement system error of 0.5%.

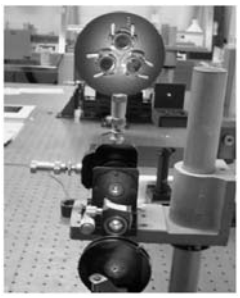

ARMs textures of the Figure 2 design are created using the two-stage lithography and etch process illustrated in Figure 4. The process begins with the patterning of an etch mask in a sacrificial material coated or deposited on the surface of the window (steps 1 thru 4), and is followed by a dry plasma etch process to transfer the mask pattern directly into the window material (steps 5 thru 7). A laser based, maskless, non-contact, large area interference lithography[20] (IL) system like the one depicted in the image on the right, was configured to generate a honeycomb array of holes or posts with a periodicity of 525nm in a photosensitive layer coated on the surface of each YAG window (steps 3 and 4).

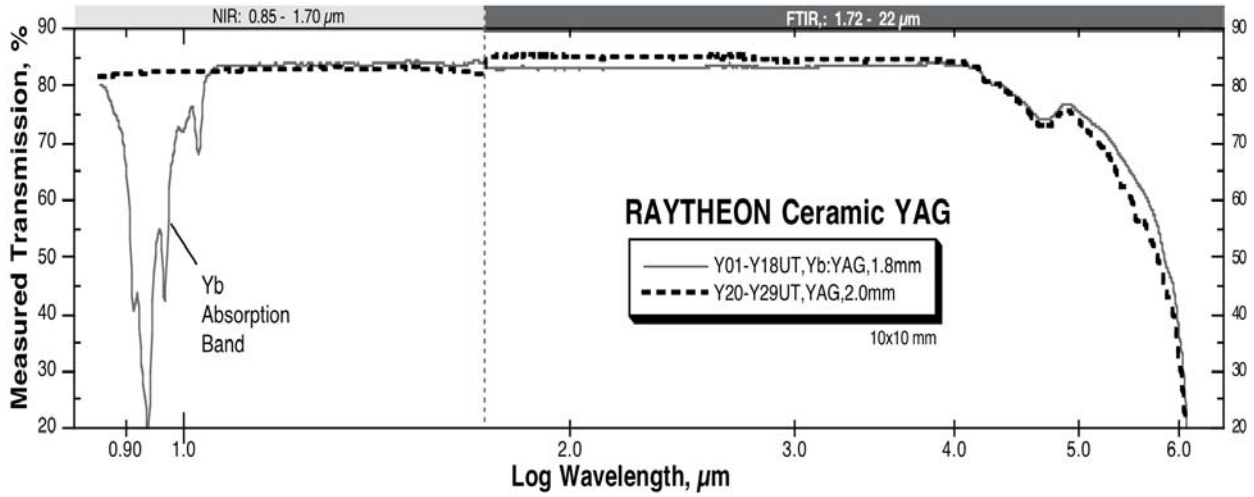

Figure 3: Measured IR transmission of 1.8 and 2.0mm thick Raytheon ceramic YAG windows prior to ARMs fabrication.

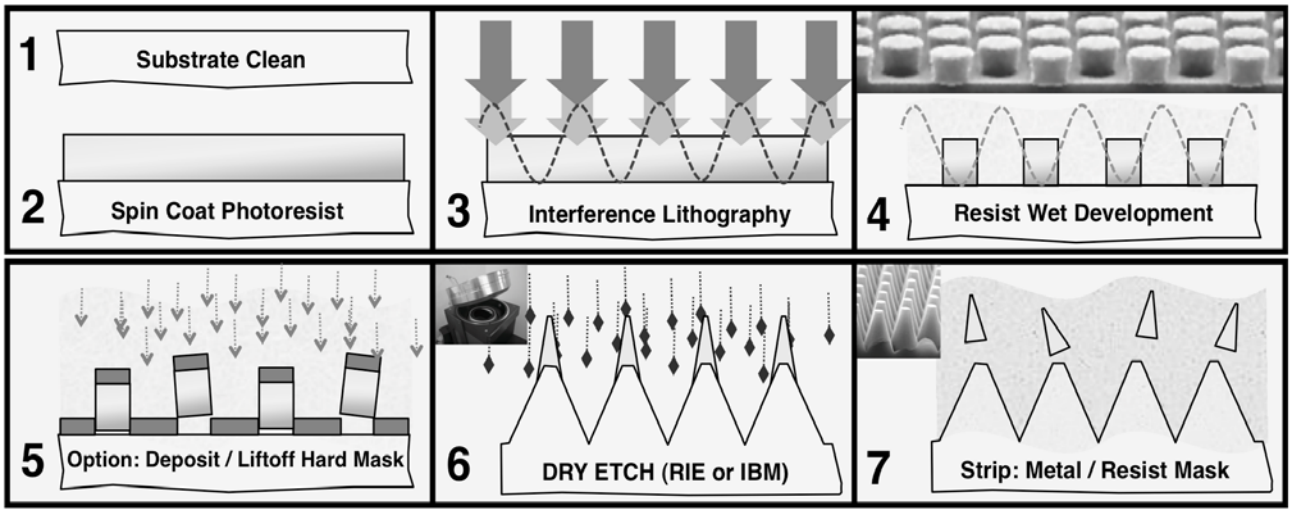

Figure 4: Process flow diagram for the fabrication of ARMs textures in a window or optic surface.

Etching microstructures in the surface of such a mechanical durable and chemically resistant material as YAG is a major challenge. A wide search of the literature did not produce any potential plasma etch chemistries for yttrium aluminum garnet, in fact only references to the etching of yttrium oxide and aluminum oxide thin-films could be found[21-23]. To verify the assumption that a simple physical etch process based on ion bombardment would not be practical, one YAG sample was patterned with a photoresist mask as described above and etched by argon ion milling. The milling rate for YAG was found to be less than 3nm/min which would require between 100 and 200 minutes of milling through a similarly low milling rate etch mask material such as silicon oxide. The alternative was to use an in-house inductively coupled plasma (ICP) reactive ion etch (RIE) system that has been capable of etching sapphire and ALON ARMs textures at rates up to 45nm/min. The fluorine based gases and high plasma energies used in the sapphire RIE/ICP processes remove photoresist at a very high rate, and therefore the typical photoresist etch masks defined by the IL process must be converted to a more durable material such as titanium or nickel. Figure 5 shows scanning electron microscope (SEM) images of the typical hole pattern created by the IL process as an intermediate step in the process of defining a hard metal etch mask (step 5 in Figure 4). The metal required is deposited by evaporation or sputtering methods over the photoresist pattern and onto the YAG substrate that is exposed at the bottom of each hole. A wet chemical liftoff process is then used to rapidly dissolve the photoresist and lift off the metal layer that was deposited on top of the resist – leaving an array of metal pads like those shown in the SEM image of Figure 6.

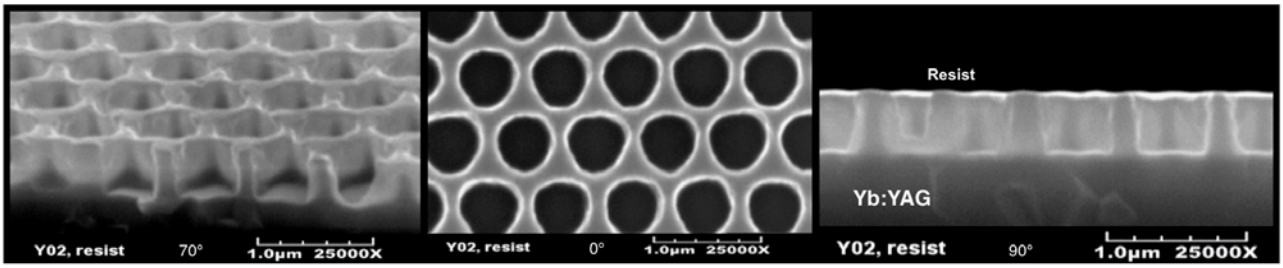

Figure 5: Elevation (70°), overhead (0°), and profile (90°) SEMs of an ARMs patterned resist mask layer on a YAG crystal.

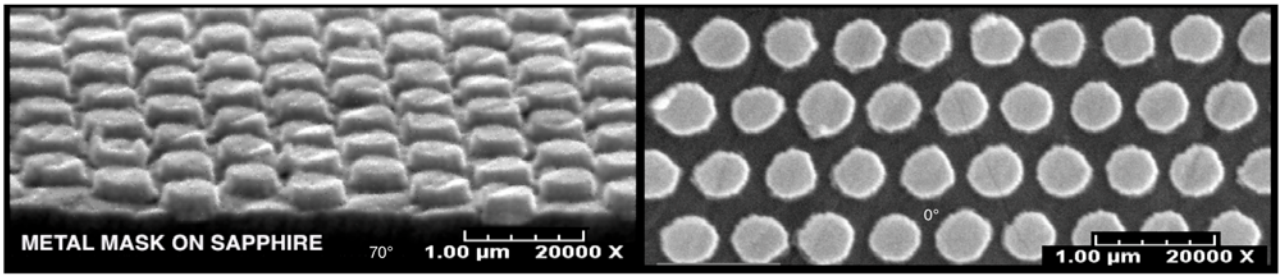

Figure 6: Elevation (70°), and overhead (0°) SEMs of an ARMs patterned metal mask layer on a sapphire window.

After metallization, an exhaustive series of etch trials were conducted using the seven fluorine and bromine based gases available in the RIE/ICP tool, and beginning with the successful parameter set used for defining ARMs textures in sapphire and ALON. These trials met with little to no success producing only physical ablation of the YAG material at rates similar to ion milling, indicating that the chemical bonds in yttrium aluminum garnet were much harder to break than the aluminum oxide bonds in sapphire. With such low chemical activity, the composition and thickness of the metal hard mask became critical. After several cycles of metal deposition, etching, stripping, and re-work, an etch process based on maximizing the ICP power and minimizing the chamber pressure yielded etch rates for YAG that were in the 10 to 15nm/min range with comparable metal mask ablation rates. These rates and mask-to-YAG etch selectivity were sufficient to generate the binary SWS-type ARMs textures as well as the tapered mesa HYBRID-type ARMs textures. Figure 8 shows SEM images of the SWS-type ARMs texture etched in the surface of an un-doped YAG sample used for process development. Further process optimization is expected to yield the cone structures needed for improved wide bandwidth performance.

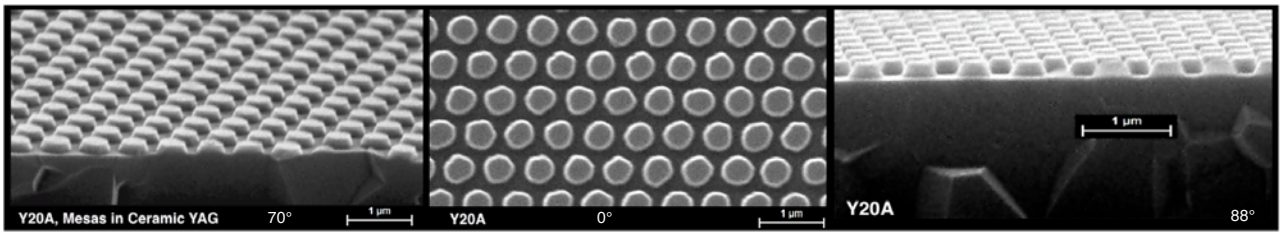

Figure 7: Elevation (70°), overhead (0°), and profile (90°) SEMs of ARMs etched in the surface of a Raytheon YAG crystal.

The performance attained with these first YAG ARMs textures was established with reflection and transmission measurements made with the NIR grating based spectrometer described above. Figure 8 is a plot showing the transmission of the samples submitted to the pulsed laser damage testing where the data has been normalized by referencing each trace to the single surface transmission established by the optical material constants given in the literature[8]. Measurements for the untreated YAG windows are relatively flat over the 1.1 to 1.7µm range and normalized at 91-91.5%. Two Yb-doped YAG windows processed with ARMs textures and labeled Y13ME and Y11ME, are represented by the black dashed and dotted curves in the figure respectively. An un-doped ARMs-textured window Y26ME is shown as the solid grey curve in the figure notable due to the lack of short wave transmission loss caused by the Yb absorption present in the doped samples. The ARMs textured samples show a modest transmission increase over the untreated windows due to the limited etch depth attained with the process as described above – a problem which will be resolved with future etch process development work.

Two additional Yb-doped YAG windows were sent to a thin-film AR coating service provided by Quality Thin Films, Inc. of Oldsmar Florida (QTF). QTF applied their proprietary high damage threshold single layer AR coating by ion beam assisted deposition, targeting maximum transmission at 1064nm. The coating performs well with less than 0.3% reflectance measured at the target wavelength and a 0.1% minimum reflection measured at 1030nm. In transmission the thin film coated Yb-doped YAG windows labeled Y16TF and Y18TF and represented by the solid black curve in Figure 8, show a value of just under 99% at 1064nm due to the roll off in the proximity of the Yb absorption band.

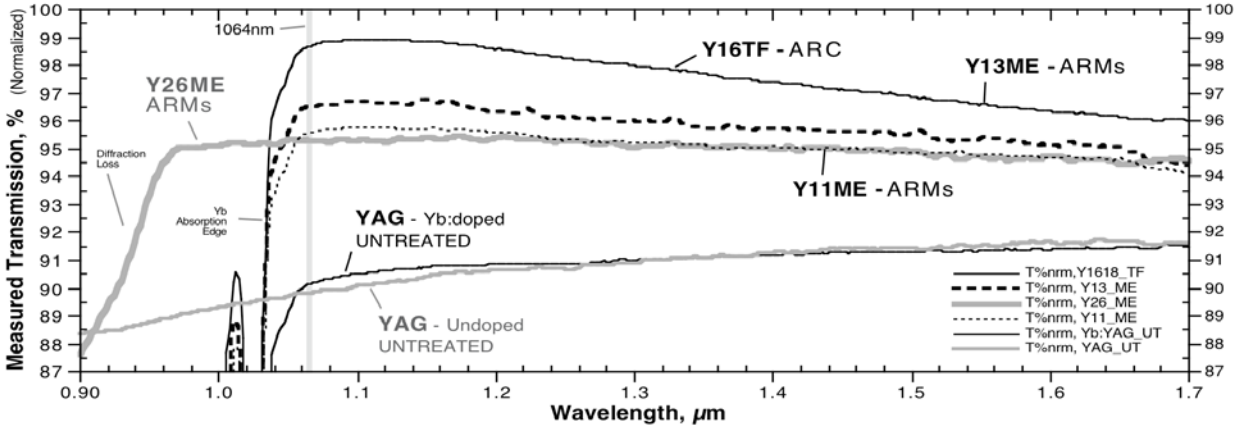

Figure 8: Measured single surface transmission of NIR light through ARMs treated and thin-film coated YAG windows.

Established RIE/ICP etch processes were used to define both HYBRID-type and Motheye-type ARMs textures in one surface of one-inch round, 6mm thick optical grade sapphire windows (99.99% purity) purchased from Crystal Systems, Inc. of Salem Massachusetts. The windows were polished on both sides to a 60-40 scratch-dig specification with a flatness of better than two waves measured in the red at 633nm. Figure 9 shows SEM images of the two types of ARMs textures produced in sapphire windows used for process witness samples. On the left are elevation and overhead views of the HYBRID ARMs texture where the tapered flat-top mesa structures are about 550nm high. Cone structures in the Motheye texture shown on the right side in the figure are about 750nm high and extend over the full period at the base for a high fill factor. The variable cone height is a result of over-etching this witness sample and was not observed in the parts submitted for laser damage testing.

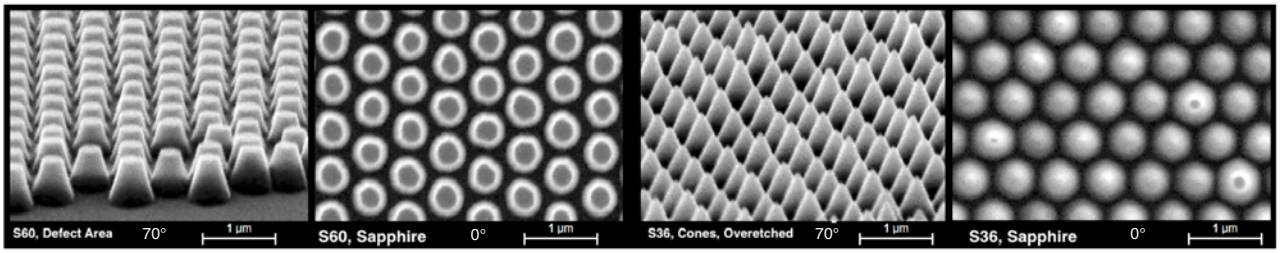

Figure 9: Elevation (70°) and overhead (0°) SEMs of NIR ARMs textures etched in the surface of two sapphire windows.

Figure 10 is a plot showing the measured transmission of the sapphire samples submitted to the pulsed laser damage testing where as with the YAG data in Figure 8, the data has been normalized by referencing the single surface transmission established by the widely published sapphire optical material constants. Two untreated sapphire windows, S42UT and S44UT, show a flat transmission between 92.5 and 93% over the NIR spectrometer measurement range. Motheye samples S30ME and S22ME represented by the black dashed and dotted curves in the figure exhibit broad-band transmission averaging better than 99.5% over the 0.92-1.7μm range shown, with a transmission maximum at the target 1064nm wavelength. A third Motheye window S32ME (thin solid black curve) has reduced performance but was processed with a high degree of uniformity and a low defect count that is expected to be important for laser damage resistance. Lastly, two sapphire windows were coated with the same single layer AR treatment applied to the YAG windows by QTF, Inc. Because the refractive index of sapphire is lower than that of YAG, the thin film coated window samples S41TF and S46TF, show peak transmission at a slightly shorter wavelength near 1μm, but still retain nearly lossless transmission at the target 1064nm wavelength.

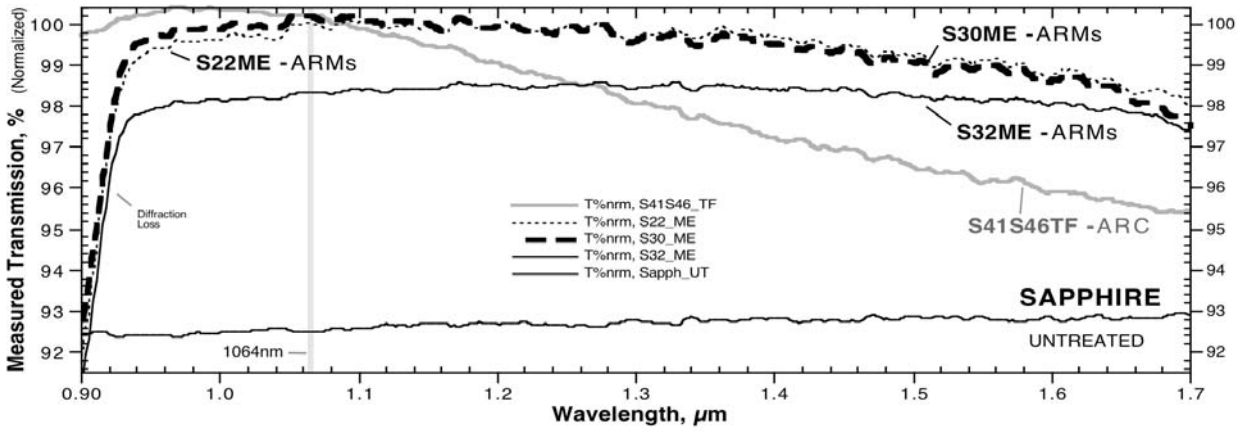

Figure 10: Measured single surface transmission of NIR light through ARMs treated and thin-film coated sapphire windows.

ALON windows provided by Surmet Corporation were also textured with ARMs, characterized for transmission and reflection, and submitted to laser damage testing. Transmission data for two Motheye textured windows, A29ME and A30ME, are given as the black dotted and dashed curves in Figure 11. Again a thin-film AR coating was applied by QTF to an ALON window A01TF, that exhibits high transmission at the target 1064nm wavelength as shown by the solid grey curve in the figure.

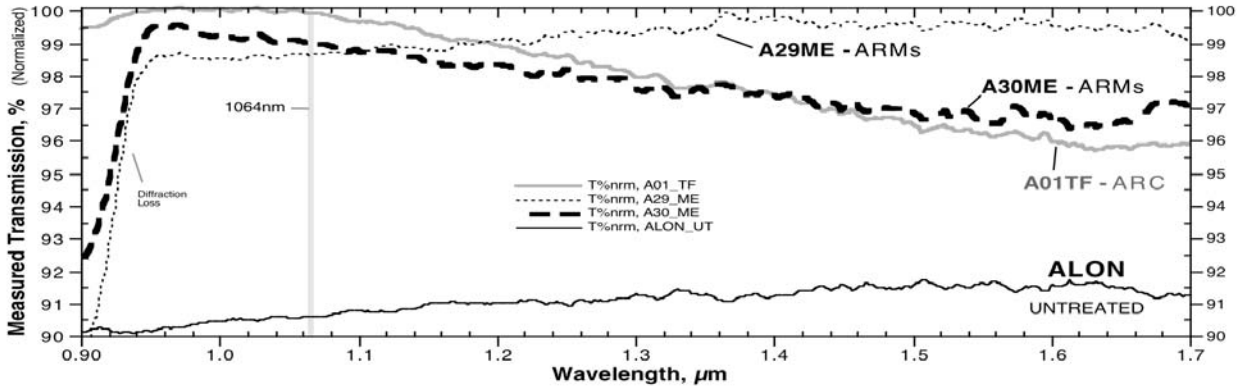

Figure 11: Measured single surface transmission of NIR light through ARMs treated and thin-film coated ALON windows.

Lastly, single crystal quartz windows were processed with ARMs textures and characterized as shown in Figure 12.

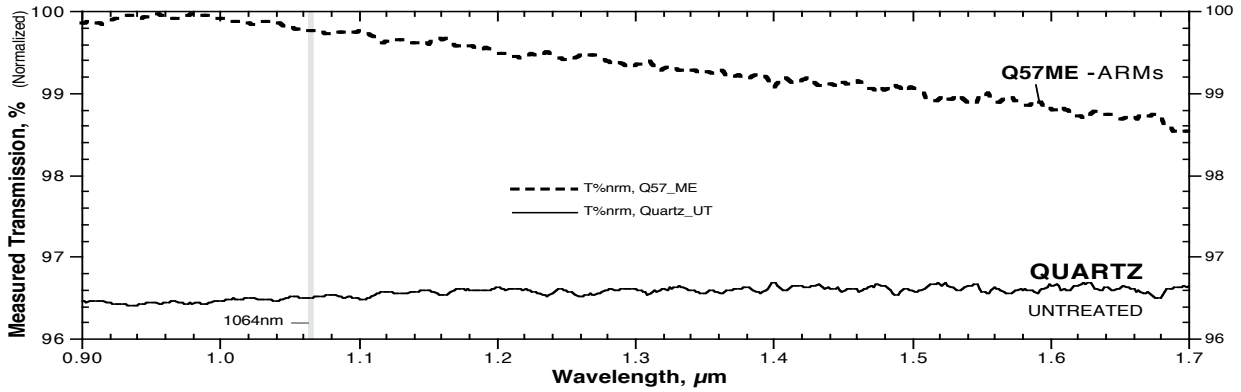

Figure 12: Measured single surface transmission of NIR light through untreated and ARMs treated Quartz windows.

4. PULSED LASER DAMAGE THRESHOLD MEASUREMENTS

At the 1064nm wavelength produced by solid state lasers based on neodymium-doped YAG, the pulsed LiDT of ARMs textures in borosilicate glass and fused silica has been shown to be as high as 57 J/cm^2 and 43 J/cm^2 respectively, values two to five times greater than the highest damage threshold values for thin-film AR coatings often reported in the literature[24,25]. To test the damage threshold of the ARMs textured YAG, sapphire, ALON, and quartz samples, the standardized pulsed LiDT testing service is provided by Quantel USA (formerly Big Sky Laser, Bozeman Montana)[26]. The tests conform to International Standards Organization (ISO) 11254, and involve exposing a statistically relevant number of discrete locations (sites) over a sample surface to a calibrated level of laser energy with a specified wavelength, pulse duration, and repetition rate. Referred to as an "S-on-1" test, the typical measurement exposes up to 100 sites to ten energy levels, 1 energy level per site to obtain a damage frequency verses energy level relationship. The criteria for damage is a permanent surface change observed by visual inspection through a microscope configured for 150X magnification. A linear fit to the damage frequency verses pulse energy data establishes the LiDT.

Pulsed LiDT measurements of untreated (UT), ARMs-treated (ME), and thin-film AR coated (TF) windows were made using a 10 nanosecond pulse width, 1064nm wavelength laser system at Quantel. Calibrated for a 420µm spot size, Quantel exposed up to 100 sites on each sample where each site received 200 pulses, or shots, delivered at a rate of 20 pulses each second. Between 9 and 12 fluence levels were distributed amongst the 85-100 exposure sites over the sample surface. Beginning with the ceramic YAG samples, two Yb-doped untreated samples (Y14UT and Y15UT) were tested along with one untreated YAG window with no doping (Y29UT). Other than standard cleaning with solvents and oxygen plasma, no special surface preparation method was used on the untreated YAG windows. Also tested were two ARMs-treated Yb-doped YAG windows (Y11ME and Y13ME) and one ARMs-treated window with no doping (Y26ME), and two Yb-doped YAG windows with thin-film AR coatings (Y16TF and Y17TF). The results from each type of sample (UT, ME, TF) were averaged, and a linear fit to the data was made to obtain the curves shown in Figure 13. A damage threshold of 11.0 J/cm^2 was measured for the ARMs treated YAG samples (solid black line/triangles), and a lower value of 7.3 J/cm^2 was measured for the untreated YAG windows (solid grey line/open crosses) – no significant difference was found between the doped and un-doped samples of each type. The low threshold for damage found with the untreated YAG windows may be due to the simple commercial polish used to prepare the windows. A more thorough polish may be needed to minimize sub-surface mechanical damage followed by what is becoming standard practice in the high power laser component industry – a chemical etch to enhance the laser damage resistance[27]. Residual sub-surface damage may have been partially removed by the plasma and wet chemical etch processes used to form the ARMs textures in the YAG windows, possibly explaining why the ARMs textured sample damage threshold was 50% higher than the untreated samples. Sub-surface damage may also have been shielded by the additional material layer deposited on the thin-film AR coated samples, leading to the high damage threshold of 21 J/cm^2 observed for both Y16TF and Y17TF (open grey squares/dashed line).

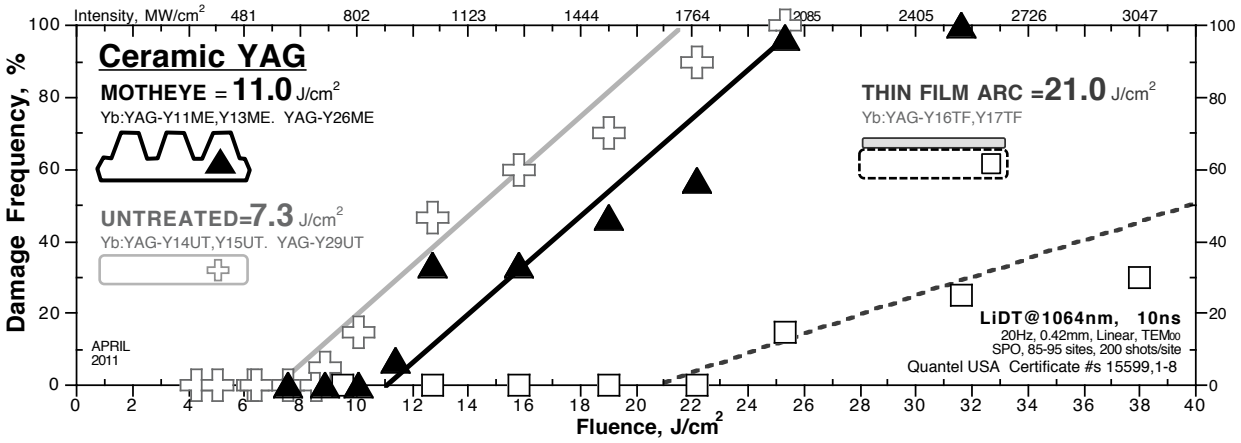

Figure 13: Results of a 1064nm LiDT test of untreated, ARMs-treated, and thin-film coated ceramic YAG windows.

The sapphire samples tested began with a much higher level of polish as provided by Crystal Systems, possibly leading to the significantly higher damage thresholds measured. Two untreated sapphire windows (S42UT and S44UT), three ARMs textured windows (S22ME, S30ME, and S32ME), and two thin-film AR coated windows (S41TF and S46TF) were submitted for 1064nm damage testing at Quantel. Figure 14 shows the results where the thresholds for the ARMs textured (solid black line/triangles) and untreated (solid grey line/open crosses) windows are comparable at 24.9 J/cm^2

and 27.5 J/cm^2 respectively. The thin film AR coated samples fared worse with a damage threshold of 16.7 J/cm^2 - about two-thirds the level of the Motheye samples.

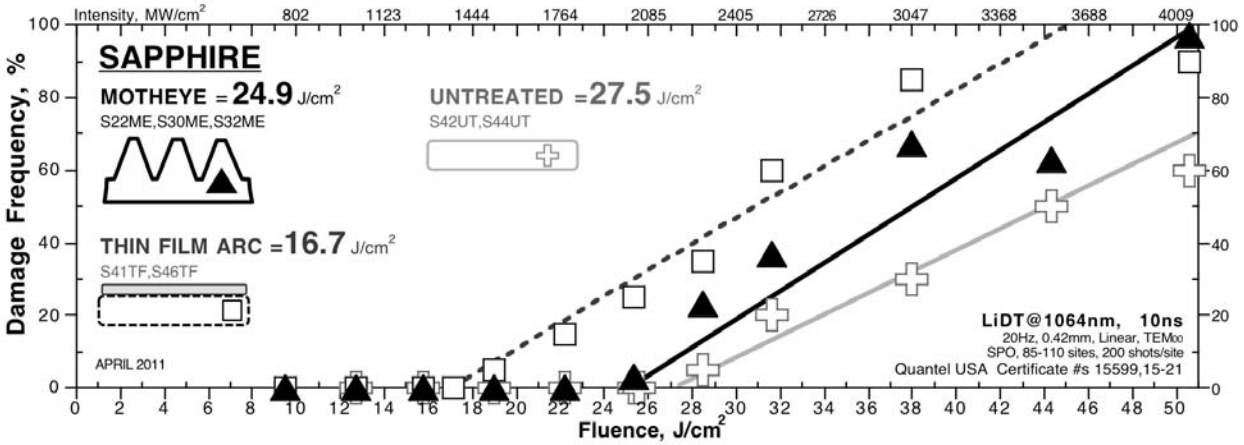

Figure 14: Results of a 1064nm LiDT test of untreated, ARMs-treated, and thin-film coated sapphire windows.

Four ALON windows and two Quartz windows were also damage tested at Quantel. The damage thresholds measured for ALON are low compared to the sapphire, a result that may also be related to un-mitigated sub-surface polishing damage. The single crystal quartz windows fared well with Motheye and untreated damage levels of 22.4 J/cm^2 and 22.8 J/cm^2 respectively. A chart summarizing all the damage testing results grouped by material, is given in Figure 15.

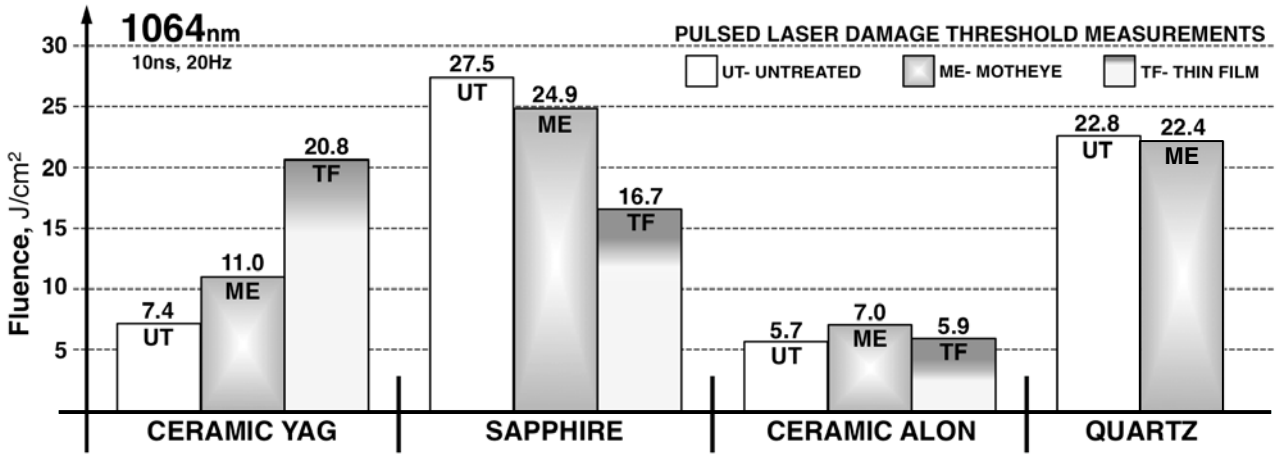

Figure 15: Bar chart comparing the 1064nm LIDT results for the four materials tested.

5. SUMMARY

As an alternative to thin-film AR coating technology, AR microstructures continue to exhibit laser damage resistance that can be equivalent to the durability of untreated material, levels 2 to 5 times higher than single or multi-layer AR coatings. Studies focused on ARMs textures built in Raytheon ceramic YAG, show that surface polishing methods and chemical etching prior to ARMs processing is critical for attaining the highest laser damage resistance. ARMs textures in highly polished sapphire and quartz materials were produced with high transmission over a broad bandwidth in the NIR combined with high levels of pulsed laser damage resistance measured using 10ns pulses at 1064nm. With further work, ARMs technology can significantly enhance the power handling capacity and reliability of solid state lasers.

5. ACKNOWLEDGEMENTS

The authors thank Jeff Runkel of Quantel USA (JRunkel@quantelusa.com) for his fast and thorough work providing the certified, NIST traceable LIDT testing results on more than 20 samples in less than 2 days. The SEM analysis was performed by Mr. John Knowles at MicroVision Laboratories, Inc., (978-250-9909).

6. REFERENCES

[1] Huie-Imholt, J., and Gentilman, R.L., “YAG Solid State Laser Ceramics Breakthroughs At Raytheon”, Raytheon Technology Today, Issue 2 (2010)
[2] Huie, J.C., "Raytheon Ceramic YAG Material Development for Laser Gain and IR Windows Application," ASSP, Nara Japan, paper WC4, (2008)
[3] Schmitt, R.L. and Do, B.T., “Design and Performance of a High-Repetition-Rate Single-Frequency Yb:YAG Microlaser”, Proc. SPIE **6871**, 687105, (2008)
[4] Huie, J.C., Dudding, C.B., and McCloy, J., “Polycrystalline yttrium aluminum garnet (YAG) for IR transparent missile domes and windows”, Proc. SPIE **6545**, 65450E (2007).
[5] Huie, J.C., Gentilman, R.L., and Stefanik, T.S., "Domestically produced ceramic YAG laser gain material for high power SSLs", Proc. SPIE **6552**, 65520B (2007)
[6] Ostby, E., Ackerman, R.A., Huie, J.C., and Gentilman, R.L., "Ceramic Yb:YAG microchip laser", Proc. SPIE **6100**, 610004 (2006)
[7] Lyngnes, O., “High Laser Damage Coatings on YAG Using Ion Beam Sputtering Deposition”, Proc. SSDLTR Laser-8, (2006).
[8] Thomas, M.E., et.al., “Optical properties of Nd doped and undoped polycrystalline YAG”, Proc. SPIE **6545**, 65450F (2007).
[9] Hobbs, D.S., MacLeod, B.D., “Design, Fabrication and Measured Performance of Anti-Reflecting Surface Textures in Infrared Transmitting Materials”, Proc. SPIE **5786**, (2005).
[10] Hobbs, D.S., “Laser damage threshold measurements of anti-reflection microstructures operating in the near UV and mid-infrared”, Proc. SPIE **7842**, 78421Z (2010)
[11] Bernhard, C. G., "Structural and functional adaptation in a visual system", Endeavour, **26**, 79 (1967).
[12] Clapham, P.B., Hutley, M.C., "Reduction of lens reflexion by the 'Moth Eye' principle", Nature, **244**, 281 (1973).
[13] Thornton, B.S., "Limit of moth's eye principle and other impedance-matching corrugations for solar-absorber design." JOSA, **65** (3), 267 (1975).
[14] Wilson, S.J., Hutley,M.C., "The optical properties of 'moth eye' antireflection surfaces", Optica Acta, **29,** 7 (1982).
[15] Lowdermilk, W.H. and Milam, D., “Graded-index antireflection surfaces for high-power laser applications”, Appl. Physics Letters, **36** (11), 891 (1980).
[16] Cook, L.M., et.al., “Integral Antireflective Surface Production on Optical Glass”, Journal of the American Ceramic Society, **65** (9), c152 (1982).
[17] Southwell, W. H., "Pyramid-array surface-relief structures producing antireflection index matching on optical surfaces", JOSA A, **8** (3), 549 (1991).
[18] Hobbs, D.S., MacLeod, B.D., “High Laser Damage Threshold Surface Relief Micro-Structures for Anti-Reflection Applications”, Proc. SPIE **6720**, 67200L (2007).
[19] Hobbs, D.S., “Study of the Environmental and Optical Durability of AR Microstructures in Sapphire, ALON, and Diamond”, Proc. SPIE **7302**, 73020J (2009).
[20] Hobbs, D.S., et. al., “Automated Interference Lithography Systems for Generation of Sub-Micron Feature Size Patterns”, Proc. SPIE **3879**, 124 (1999).
[21] Bradley, J.D.B., Ay, F., Wörhoff, K., and Pollnau, M., “Fabrication of low-loss channel waveguides in Al2O3 and Y2O3 layers by inductively coupled plasma reactive ion etching”, Appl. Phys. B, **89** (2), 311 (2007)
[22] Kim, M., “Effect of Gas Mixing Ratio on Etch Behavior of Y_2O_3 Thin Films in Cl_2/Ar and BCl_3/Ar Inductively Coupled Plasmas”, Japanese J. Appl. Phys. **49** (8), (2010)
[23] Bernhardi, E. H., “Highly efficient, low-threshold monolithic distributed-Bragg-reflector channel waveguide laser in Al_2O_3:Yb^{3+}”. Optics Letters **36** (5) (2011)
[24] Stolz, C. J., Adams, J., Shirk, M. D., Norton, M. A., Weiland, T. L. “Engineering meter-scale laser resistant coatings for the near IR (LLNL)”, Proc. SPIE **5963**, (2005)
[25] Ciapponi, A., et.al., “S on 1 testing of AR and HR designs at 1064 nm”, Proc. SPIE **7842**, 78420J (2010)
[26] Quantel USA, “Optical Damage Testing”, http://www.optical-damage-testing.com/en/
[27] Miller, P. E., et.al., "Laser damage precursors in fused silica," Proc. SPIE **7504**, 75040X (2009).